



Science Arts & Métiers (SAM)

is an open access repository that collects the work of Arts et Métiers Institute of Technology researchers and makes it freely available over the web where possible.

This is an author-deposited version published in: <https://sam.ensam.eu>
Handle ID: <http://hdl.handle.net/10985/9894>

To cite this version :

Monir ASGARPOUR, Alireza KHAVANDI, Abbas TCHARKHTCHI, Farid BAKIR, Sofiane KHELLADI - 3D Model for Powder Compact Densification in Rotational Molding - Polymer Engineering and Science - Vol. 52, p.2033-2040. - 2012

Any correspondence concerning this service should be sent to the repository

Administrator : scienceouverte@ensam.eu



3D Model for Powder Compact Densification in Rotational Molding

Monir Asgarpour,¹ Farid Bakir,² Sofiane Khelladi,² Alireza Khavandi,³ Abbas Tcharkhtchi¹

¹ PIMM, Arts et Métiers ParisTech, 151 Bd de l'Hôpital, Paris, France

² DynFluid, Arts et Métiers ParisTech, 151 Bd de l'Hôpital, Paris, France

³ Material Engineering Department, IUST, Tehran, Iran

During rotational molding, a loosely packed, low-density powder compact transforms into a fully densified polymer part. This transformation is a consequence of particles sintering. Powder compact density evolution of the polymer powder is measured experimentally. Obtained results show that the powder densification process consists of two stages, and its mechanism during these two stages is not the same. During the first stage, densification occurs by grains coalescence, and air between the grains escape by open pores between particles. These open pores close in time by particles coalescence progress, and remaining air entrapped in polymer melt becomes air bubbles. Surface tension, viscosity, grains size, and temperature are the controlling parameters during first stage. A three-dimensional model is proposed for the densification of polymer powder during first stage. Second stage starts after bubble forming. Diffusion is the controlling phenomena during this stage. A diffusion-based model is used for the second stage of densification. By comparing with the other models, proposed model exhibits several advantages: it is proposed in three-dimensional and takes into account the nature of layer-by-layer powder densification. Model verification by experimental data obtained for densification of two different polymers shows a close agreement between model prediction and experiments. POLYM. ENG. SCI., 52:2033–2040, 2012. © 2012 Society of Plastics Engineers

INTRODUCTION

Rotational molding is a relatively inexpensive method used originally for manufacturing of hollow parts like toys, storage drums, and other products. The major difficulty faced during its application for the manufacturing of industrial parts with complicated geometry was to control their thickness and surface quality and also the presence of air

bubbles in the material. The work done by research community, during past many years, has improved the process capacity, and still a lot of work is being done to understand the material behavior during actual molding process.

In rotational molding, polymer is introduced in powder form into a mold, which rotates biaxially. This powder is then heated, and once it reaches the melting point temperature, the grains start to melt and stick to the mold surface and to each other. As the melting process continues, the grains start to fuse, and this process is called coalescence. Interspace distance between the grains reduces due to their coalescence. The result is the change of density, and this phenomenon is called densification of powder. "Sintering" is the term accepted in the material science literature for the combined action of coalescence and densification.

Polymer is used in powder form in many industries like rotational molding. In this case, the bulk density of polymer powder is low due to the very high quantity of air between the grains. During rotational molding, powder melts freely, and there is not any external force except gravity to allow the release of air between the grains. The remaining air that becomes air bubbles reduces the mechanical properties and the surface quality of the final product part. So, sintering is not only inherent in rotational molding process but also is the controlling phenomenon.

Densification mechanism changes during rotational molding process. The air between the powder particles exits in two steps during sintering of grains:

When the grains adhere to each other during sintering, the free spaces between the grains reduce, and the air between the grains exits by the free spaces between them.

Once these free spaces are closed, the remaining air is trapped in the polymer melt (air bubbles formation). After bubble formation, densification occurs by gas diffusion into polymer.

The effect of different parameters, like temperature, viscosity, and powder characterization on the powder densification has been studied. But the approach has primarily been experimental. There are not many models

Correspondence to: Monir Asgarpour; e-mail: m_asgary2002@yahoo.com

DOI 10.1002/pen.23133

describing powder densification during rotational molding, and the few existing models permit only a partial analysis of phenomena.

During rotational molding, coalescence and densification of powder are done in a three-dimensional network. So, a three-dimensional model is needed to describe this phenomenon. This model must take into account the melting of polymer and the migration of gas in molten polymer with time during processes.

In this work, using the grains sintering model, a three-dimensional model was proposed for powder compact densification. This model is then verified by densification experimental results obtained for two different polymers.

BACKGROUND

Air bubble presence in the viscous materials has been first recognized in the glasses [1]. Even this problem is not limited to glass and ceramics industries, but is not a common problem of polymer industries. So, there are not many studies done on polymer densification and air bubbles formation and removal in polymers.

There are different hypotheses about bubbles formation during powder densification. Rao and Throne [2] have affected the first study on the polymer powder densification. They considered that the formation of a homogeneous polymer melt from powder grains was done in two stages: first, the grains fuse to each other and with the growth of the interface between them, a three-dimensional network forms between them. In the second step, this three-dimensional network collapses, and the polymer melt fills the free spaces between the grains. At a slow sintering rate, air bubbles have enough time to move toward the polymer-free surface; otherwise, they remain in the polymer melt layer. Concerning the bubbles, Kelly [3] observed that, once they are formed in the melt, they remain stationary and do not move.

Later, Kontopoulou and Vlachopoulos [4] proposed a model for three-dimensional densification of powders based on the formulation proposed by Scherer [5]. Their model is proposed for isothermal conditions. During their studies, Kontopoulou and Vlachopoulos [4] observed that the densification of polymer powder occurs layer by layer. But, in their proposed model, they considered that the sintering of all the grains happens simultaneously. This is far from real condition of rotational molding.

To take into account the layer-after-layer densification reality, Bellehumeur and Tiang [6] proposed another model. They considered thickness of each layer equal to average diameter of the powder particles. Heat transfer model was used to predict the rate at which each layer of powder deposits on the mold surface. In their model, they considered two idealized arrangements of equal size particles (simple cubic and face-centered cubic) in two dimensions. In this model, the sintering time for a particle of the n th layer was defined as the time required for the melt deposition front to go from the n th layer up to $(n +$

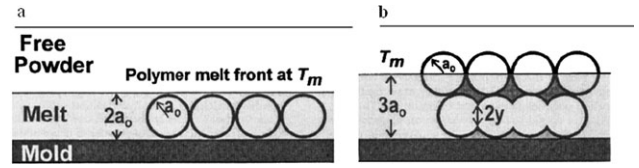


FIG. 1. (a) Schematic representation of melt deposition and (b) bubble formation.

$1/2$)th melt layer (Fig. 1) [6]. This time corresponds to the time during with the particles of n th layer coalesce to each other, and so the free spaces between the grains of two layers decrease. These spaces correspond to the cavities between the particles, and their surface changes with particle sintering resulting in changes of the powder density.

Using sintering model, they calculated the initial area of cavity formed between two layers of particles. This area changes with time until next layer reached melting point. At this moment, it remains constant. This fixed area corresponds to the formation of first bubble surface between the grains. According to this hypothesis, the level of coalescence between particles, the size of the particles, and the packing arrangement dictate the size of the air cavities. First size of air cavities corresponds to the initial size of air bubbles. As this model was proposed in two dimensional, compared to the real three-dimensional powder densification, application of this model can introduce the errors into the calculation. It is not able to explain the mechanism of air bubbles formation in three-dimensional powder bulks.

Bubbles' size changes by gas diffusion into polymer melts after their formations [7–9]. By balancing three forces acting on the bubble, Gogos [10] calculated the terminal velocity of a rising bubble. Different studies show that bubble rising velocity in rotational molding for an average size bubble is negligible [3, 8, 11], and it can be considered stationary in a polymer melt.

Cell model [4] is one of the used methods for the prediction of a single bubble life in a polymer melt. This model considers that each bubble is contained within a spherical fluid cell of radius R_{cell} (see Fig. 2). Using this model and by solving the diffusion, conservation of momentum, and continuity equations simultaneously, Kontopoulou and Vlachopoulos [7] proposed a model (Eq. 1) for bubble diameter changes by time. In this model, the force balance around the bubble has been taken into account.

$$R_{\text{cell},0}^3 - R_0^3 = [R(t)]_{\text{cell}}^3 - [R(t)]^3 \quad (1)$$

where R and R_{cell} are the gas bubble radius and cell radius, respectively (see Fig. 2). R_{cell} and $R_{\text{cell},0}$ are new values of R and R_{cell} after every time step. By comparing this model with experimental results, Kontopoulou and Vlachopoulos observed a significant difference between model's prediction and experiments. According to them, this is because they did not consider the fact that polymer densification occurs layer by layer.

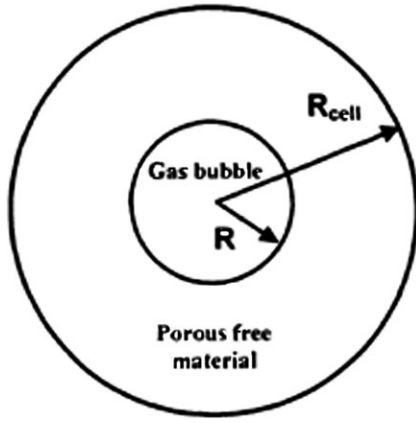


FIG. 2. Schematic of a gas bubble contained within a spherical cell of radius R_{cell} .

Another model for modeling the second step of densification is proposed by Gogos [10]. According to Gogos, bubble life time in a polymer depends on the melt saturation level and surface tension of polymer. Considering the effect of these parameters on the gas diffusion rate into the polymer melt, they proposed a model for bubble shrinkage with time, and they calculated the bubble life time (Eq. 2).

$$\begin{aligned}
 t_b = & \frac{\rho_{\infty}}{8D(c_{s,p_{\infty}} - c_{\infty})} R_0^2 \\
 & + \frac{\tau R_0}{3D(c_{s,p_{\infty}} - c_{\infty})} \left(1 - \frac{3}{2} \frac{c_{s,p_{\infty}}}{(c_{s,p_{\infty}} - c_{\infty})} \right) \\
 & - \frac{2\tau^2 c_{s,p_{\infty}}}{3D\rho_{\infty}(c_{s,p_{\infty}} - c_{\infty})} \left(1 - \frac{3}{2} \frac{c_{s,p_{\infty}}}{(c_{s,p_{\infty}} - c_{\infty})} \right) \\
 & \ln \left[1 + \frac{\rho_{\infty}(c_{s,p_{\infty}} - c_{\infty})R_0}{2\tau c_{s,p_{\infty}}} \right] \quad (2)
 \end{aligned}$$

where R_0 is the bubble initial diameter and D is the diffusion coefficient (m^2/s) of gas in the polymer. C_{∞} and $C_{s,p_{\infty}}$ are the dissolved gas concentration in the melt when partially saturated and saturated for zero-surface tension. τ is surface tension coefficient of polymer and ρ_{∞} is the pressure in the bulk of the melt.

By verifying Gogos's model, Kontopoulou and Vlachopoulos [7] have shown that the effect of viscosity is negligible when compared with the surface tension. Comparing

Gogos's model with the experimental results, Bellehumeur and Tiang [6] observed a good accord.

MATERIALS AND METHODS

Two different polymers were used during this work: polypropylene (PP), supplied by ICO POLYMERS, and polyvinylidene fluoride (PVDF), supplied by Solvay company. Both of them were used in powder form comprising spherical particles (Fig. 3). The sizes of PP and PVDF grains range from 100 to 600 μm and 20 to 100 μm , respectively. Dynamic viscosities of these polymers were measured by an ARES rheometer (from TA Instruments Company) using parallel plates with a gap of 1 mm under nitrogen to avoid degradation. Thermal properties were determined by differential scanning calorimetry Q10 from TA instrument©.

Surface tensions of these polymers were measured at different temperatures by using a drop-shape analysis system DSA100 from KRÜSS©.

To monitoring the density evolution of a powder compact, aluminum capsules with specific dimensions (Fig. 4) are used to prepare the samples. Once the capsule is full, the excess powder is scraped off. The mass of powder is dried and then weighted by using a METTLER AT 261 balance.

Bulk density of powder is the mass of powder in a given volume without being packed. By comparing bulk density of powder with real density of polymer, air volume fractions of prepared samples were calculated.

Prepared samples are introduced in a preheated oven. Oven temperature was maintained at a constant temperature during densification experiments. Heated capsules were removed one by one at different times and quenched in cold water. Quenched samples were dried at 40°C for 10 h. Using METTLER xs203s electronic densimeter, density of dried samples was measured. Density of each sample was measured five times, and reported values are their average. The same experiment was repeated at different temperatures ($T_f + 5$, $+15$, $+25$, and $+35^\circ\text{C}$, where T_f is melting temperature). Densification experiments were repeated three times for each temperature, and average of obtained values is reported during this work.

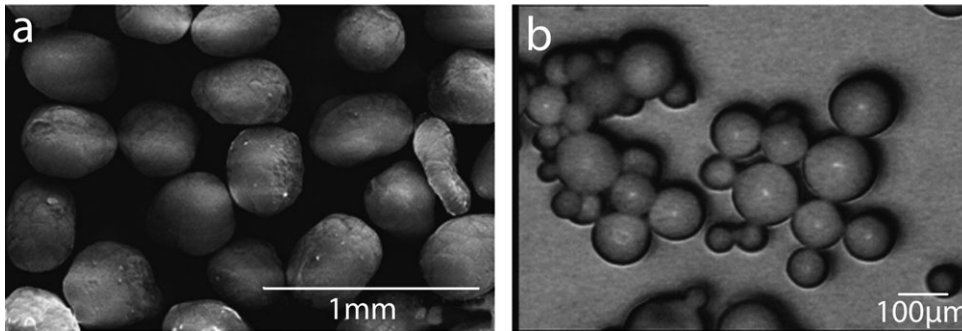


FIG. 3. Powder particles of (a) PP and (b) PVDF.

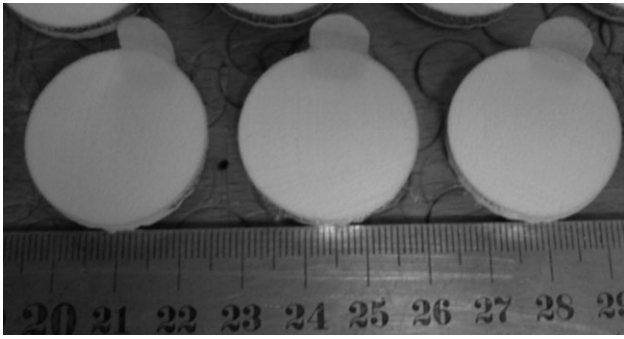


FIG. 4. Polymer densification samples.

Modeling of Densification

In fact, another parameter that must be taken into consideration is the presence of air between the grains. As explained previously, in rotational molding, the polymer is used in powder form. The diagram temperature-time (Fig. 5 [12]) gives information about the evolution of physical state of polymer during rotational molding.

On this diagram, the change of slope of the curve at point A corresponds to the melting of polymer and formation of polymer layer on internal surface of the mold. During this process, one can distinguish two following phenomena: successive formation of polymer layers one after other (Fig. 6) and coalescence of the grains. In Fig. 6, once one starts to heat the grains (steps 1 and 2), they start to melt and coalesce to each other, and the melted polymer layers form the support one after the other (steps 3 and 4). During these steps, air imprisons in the melted polymer until melting the last grain. During the next step (step 5), the air inside the bubbles diffuses into the polymer until their complete disappearance (step 6).

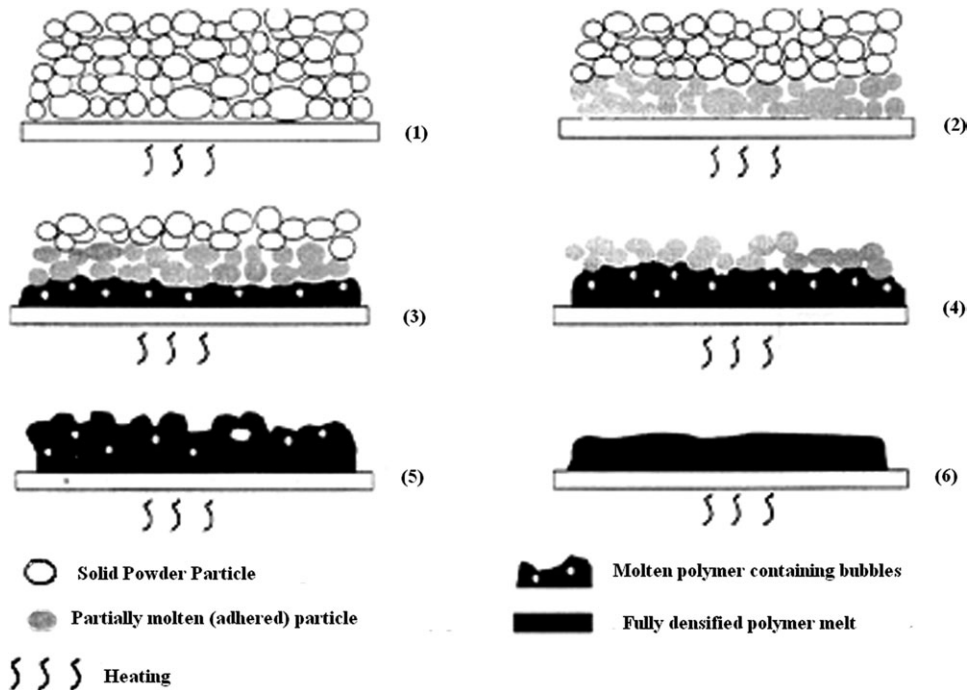


FIG. 6. Schematic of layer-by-layer densification of powder of polymer.

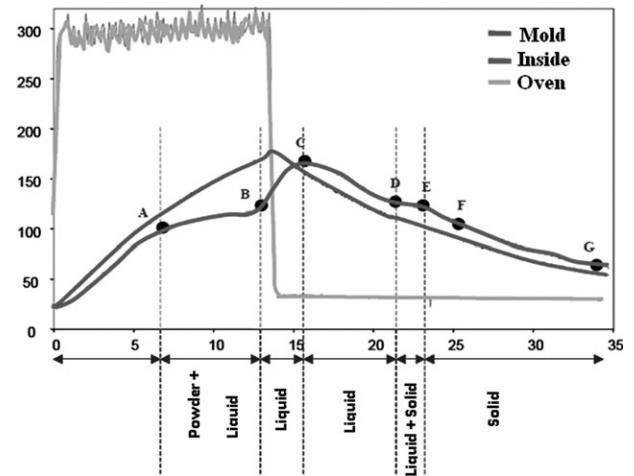


FIG. 5. Temperature-time diagram during rotational molding.

Segment AB represents the period during which all the grains of powder are transformed to the successive layers on internal surface of the mold. Coalescence is one the predominant phenomena of this period. Part AB corresponds to the first step of densification (coalescence of grains and powder volume changes). From point B to C (temperature max) and then from point C to D (beginning of crystallization), the polymer is in molten state. This period corresponds to second step of densification (diffusion and migration of gas).

Present work considers the deposition of equal-sized spherical particles arranged in a three-dimensional packed configuration. Powder characterization and particle arrangement affect the bulk density of powder. Comparing the bulk density of used powders with arrangement models [FCC (face centered cubic, HCP (hexagonal

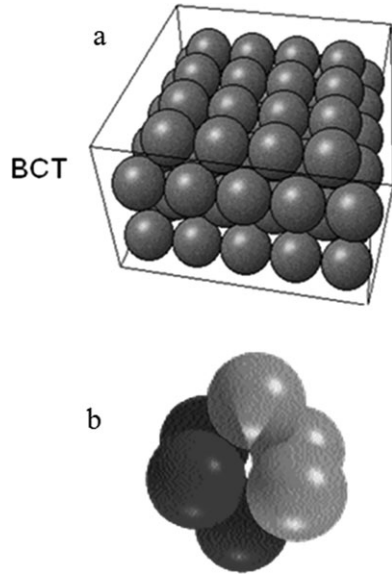


FIG. 7. (a) BCT arrangement and (b) unit cell formed between the grains in the BCT arrangement.

close-packed), BCC (body-centered cubic) ...] show that the packing of these powders is better presented by BCC and BCT (body-centered tetragonal) arrangements. BCT model is chosen to present the particles arrangement during this work. Figure 7 presents the BCT arrangement of equal-size grains. The unit cells like Fig. 7b can be detected in a BCT arrangement between grains.

Densification of this unit cell was studied during this work. Once the grains reach at melting point, they started to fuse to each other, and the free space inside the unit reduces. This reduction is due to air exiting by free spaces between the grains on the surface of unit cell in consequence of grains sintering. These free spaces between the grains of the unit's surfaces reduce in time with sintering progress. Figure 8 shows the different sections of a unit cell. The configuration of the grains on a surface of unit cell is presented in Fig. 8b.

The pits on the surface (between three grains) close earlier comparing with free spaces on the diagonal of unit cell (between four grains Fig. 8a). Once the pits on the surfaces are closed, the air between the grains of unit cell cannot escape anymore. This moment corresponds to the imprisonment of the rest of the air inside the unit cell. This phenomenon can explain the formation of the first air bubble between the grains. Using sintering laws and geometrical parameters, the volume change of unit cell is calculated with time.

Proposed Model

Heat Transfer in Powder. During rotational-molding process, the heating cycle can be divided into three regimes. First, the mold should be heated until melting point of polymer. At this time, polymer particles that are in contact with mold start to melt. During second phase, powder particles melt layer after layer, and this phase ends when there is no powder particle left. Melted poly-

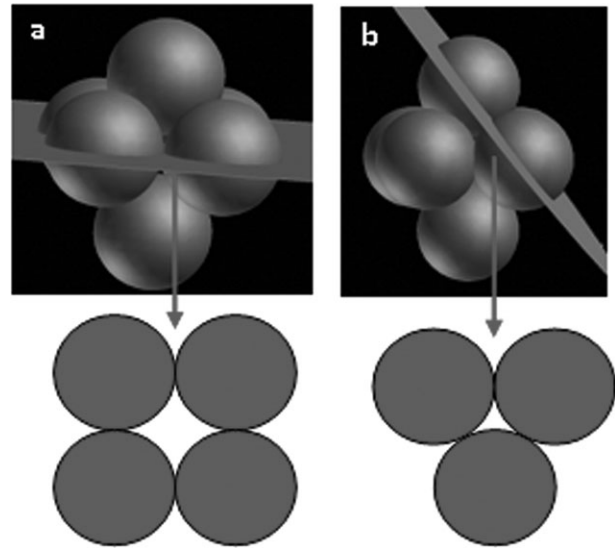


FIG. 8. Different sections of a unit cell.

mer's temperature increases during third phase. Powder densification occurs during second and third phase.

Densification of powder occurs by adhesion of grains and exiting of air between them. Powder grains should reach to melting temperature to fuse to each other. According to heat-transfer laws, the temperature of the polymer melt at the melt/powder interface is equal to the melting temperature [6]. Except for the first powder layer that is directly in contact with the mold, other layers are in contact with a melted polymer layer during their sintering. The temperature of this melted layer is equal to melting temperature. In this work, it is considered that the time needed for sintering of n th layer corresponds to time needed for melting of the particles of $n + 1$ th layer. Comparison of heat transfer calculation and experimental results of layer-by-layer polymer powder densification show that this hypothesis does not introduce considerable errors in densification calculations.

Volume Changes. Using geometrical calculations in 2D, surface change between four grains (Fig. 9) was calculated as a function of time. Obtained equation for

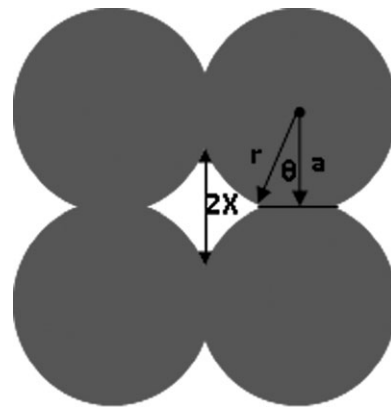


FIG. 9. Surface changes between four grains during sintering.

changes in this area used to calculate the changes in volume of unit cell with time.

Unit-cell volume changes are calculated as follows:

$$V(t) = S^3 - \left[2S^2 \left(r - \sqrt{r^2 - \left(\frac{S}{2} \right)^2} \right) \right] \quad (3)$$

where

$$S(t) = 2 \sin \theta' \quad (4)$$

$$\theta' = \left(\frac{\pi}{4} - \theta \right) \quad (5)$$

$$\theta = \arcsin \left(\frac{a - X}{a} \right) \quad (6)$$

$$r = \sqrt{a^2 + (a - X)^2} \quad (7)$$

where t is sintering time, X is the half of diagonal of the area between the grains, a is particle radius, and $S(t)$ is surface between four grains at t . X is calculated using Bellehumeur sintering model [13]:

$$8(\alpha\tau K_1 \theta')^2 + \left[2\alpha\tau K_1 + \frac{\eta\alpha_0 K_1^2}{\Gamma K_2} \right] \theta' - 1 = 0 \quad (8)$$

where

$$K_1 = \frac{\sin(\theta)}{(1 + \cos(\theta))(2 - \cos(\theta))} \quad (9)$$

$$K_2 = \frac{2^{-5/3} \cos(\theta) \sin(\theta)}{(1 + \cos(\theta))^{4/3} (2 - \cos(\theta))^{5/3}} \quad (10)$$

where a_0 is the initial radius of grains, η the viscosity, Γ the surface tension, and θ the coalescence angle.

Considering that densification of powder in the rotational molding occurs layer by layer, obtained model for the densification of unit cell can be extended to the bulk of powder. The thickness of each layer is taken to be equal to the height of the unit cell. Sintering condition is considered to be isotherm during this work.

According to the proposed model, the initial bubble diameter is determined on the basis of the volume of the closed space inside the unit cells. This volume depends on the powder grain size and their arrangement in the mold. In this model, the grains have been considered equal-sized spheres.

As the free spaces inside the unit cells close (with progress of sintering), air gets entrapped in the polymer melt by diffusion. Closed spaces between grains obtain circular form due to the action of surface tension. Densification mechanism changes after bubble formation, and this phenomenon continues by gas diffusion from air bubble into the polymer. The relative density of unit cell is defined as

the ratio of the density of the unit cell (contained closed air space inside it) to that of the polymer melt.

The model used for second step of densification (after bubble formation) is based on the analytical solution presented by Gogos [10]:

$$R_0^2 - R^2 + 2(a_2 - a_3)(R_0 - R) + 2a_3(a_2 - a_3) \ln \frac{R + a_3}{R_0 + a_3} = 2a_1 t \quad (11)$$

where

$$a_1 = \frac{D(C_{s,P_\infty} - C_\infty)}{\rho_\infty} \quad (12)$$

$$a_2 = \frac{2\tau}{3\rho_\infty} \quad (13)$$

$$a_3 = \frac{\tau C_{s,P_\infty}}{\rho_\infty (C_{s,P_\infty} - C_\infty)} \quad (14)$$

where R and R_0 are the bubble radius at time interval t and the initial bubble radius, and D is the diffusion coefficient (m^2/s) of gas in the polymer. C_∞ and C_{s,P_∞} are the dissolved gas concentration in the melt when partially saturated and saturated for zero-surface tension. τ is surface tension coefficient of polymer and ρ_∞ is the pressure in the bulk of the melt.

Surface tension and degree of saturation of polymer are the controlling parameters of gas diffusion into polymer, and so bubble life time in polymer melt depends on these parameters [10]. Once a bubble is formed, air pressure inside the bubble becomes higher than the ambient pressure, due to the surface tension of polymer in the bubble/melt interface. Difference in pressures causes the gas to get dissolved into the polymer. Gas concentration in polymer increases with time, and the degree of saturation in the melt changes. In the undersaturated condition, the surface tension effect is negligible, and the dissolved gas concentration at the bubble/polymer melt interface can be approximated as a saturated solution.

RESULTS AND DISCUSSION

The surface changes between these grains and the distance between the contacts (X in Fig. 9) were measured in time for the coalescence of four grains (Fig. 10). Obtained results were compared to model predictions in Figs. 11 and 12. The surface change in the Fig. 11 is normalized by the initial surface between four grains. Using these experimental results, the volume changes of a unit cell were calculated and compared to the model predictions. Figure 13 shows that the model prediction is compatible with the results obtained from experimental measures. Obtained results confirm that geometric calculations

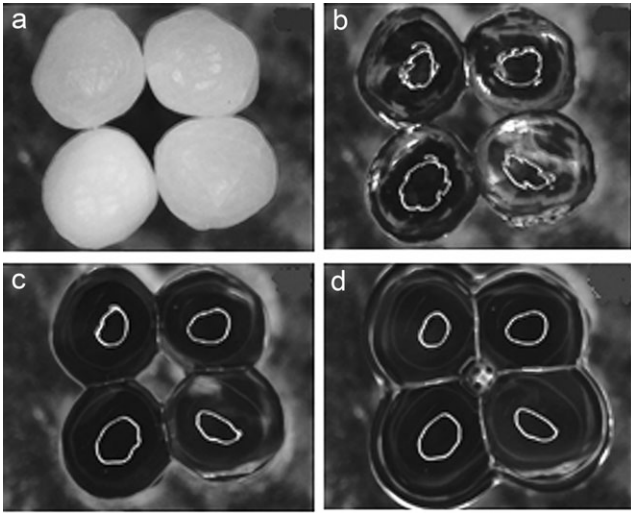


FIG. 10. Coalescence of four grains of PP at 190°C.

for first part of densification are done correctly in the proposed model.

In another part of this work, the model predictions are validated by comparing them with data obtained from densification tests done according to the method explained previously. Density evolution for PP powder is presented in Fig. 14. Comparison of the experimental results and model prediction shows that in the first stage of densification, there is a considerable gap between experimental results and model prediction. These differences can be introduced by experimental method used to density measures. The first samples exited from oven have lots of porous. Entered water into these porous during density measurements can introduce errors in obtained data. One can see in Fig. 14 that, except the first stages, the BCT model predictions are in agreement with the experiment measures.

BCT model is only valid until bubble air formations ($x/r = 0.57$). As the mechanism of densification before and after bubble formation changes, one model cannot describe both these mechanisms, and two different models are needed to model the complete processes. The BCT model that describes the densification of a powder com-

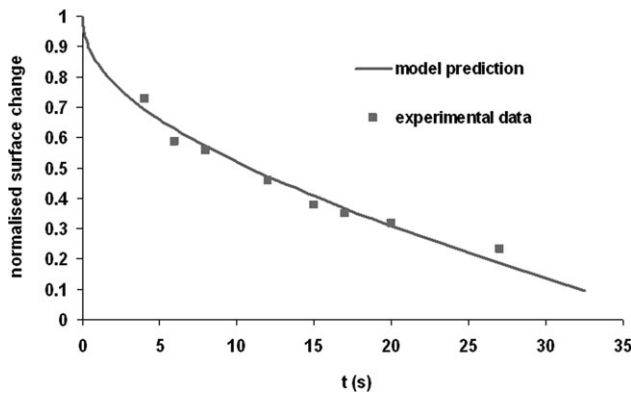


FIG. 11. Surface changes between four grains of PP during their sintering as function of time.

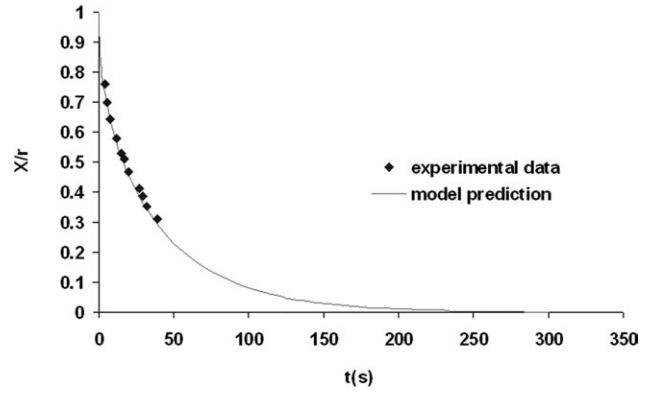


FIG. 12. Change of distance between the contacts in function of time during sintering of four PP grains.

part cannot describe the densification of polymer after bubble formation. As discussed previously, diffusion-based model was used to describe the density evolution of the polymer-containing air bubbles. The BCT model can be used only before bubbles formation ($x/r = 0.57$; Fig. 8). The initial bubble size corresponds to the volume of the free space inside a unit cell at this point and was calculated using BCT model and was used in the diffusion model.

Gogos's proposed equation for gas diffusion into polymer is solved (using numerical methods) to study the bubble size evolution in time and different material properties effects on the bubbles life time. The degree of saturation of polymers was estimated by numerical solution of the model and curve fitting. Using ideal gas law, the density of nitrogen (ρ_∞) at these ambient conditions is calculated to be 0.739 kg/m³. The ambient mass concentration c_∞ was set to zero. The mass diffusion coefficient of used polymers was obtained from polymer's handbook [14]. As explained previously, initial bubble size controlled by powder grains size and packing arrangement. Powder characteristics such as particle size distribution and their form are packing arrangement controlling parameters. Figure 15 shows the dissolution rate of three air bubbles in molten PP. The only different parameter between these three bubbles is their initial size, and other conditions are

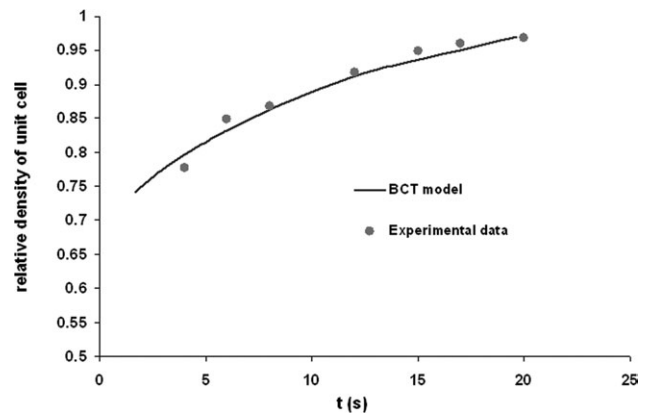


FIG. 13. Change of a PP unit cell density with time.

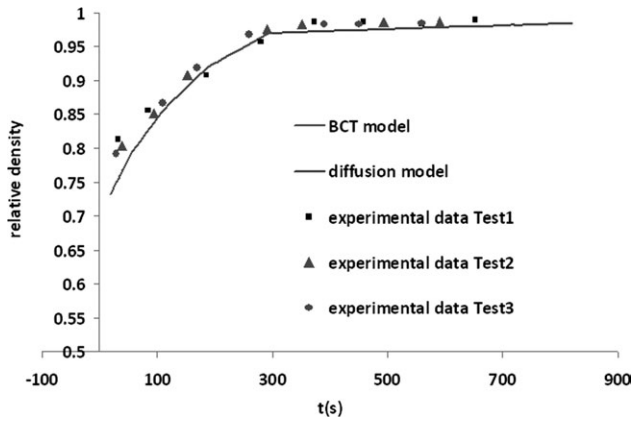


FIG. 14. Relative density of PP powder compact.

the same for all of them. Bubbles initial sizes greatly affect their life time and their dissolution rate.

Diffusion model prediction was compared to the obtained experimental data in Fig. 14. One can see that model predictions are in good agreement with the experimental data. Proposed model was verified by PVDF powder. Obtained results are shown in Fig. 16. These results confirm that proposed model can be used to predict the densification of a bulk of powder in function of time. Using this model, one can calculate the initiation size of the formed bubbles to introduce into the diffusion model.

CONCLUSION

A three-dimensional model is proposed for the densification of a powder compact during rotational molding. This model is able to describe the formation and evolution of bubbles in polymer melt during densification. A diffusion-based model was used to allow predictions of density versus time and used successfully to make prediction of the densification process, starting from the point where closed pores form. Proposed models were verified by using two different polymers powder-containing spherical particles. Obtained results show a good agreement between models prediction and experiments. According to BCT model, powder particle size and packing arrange-

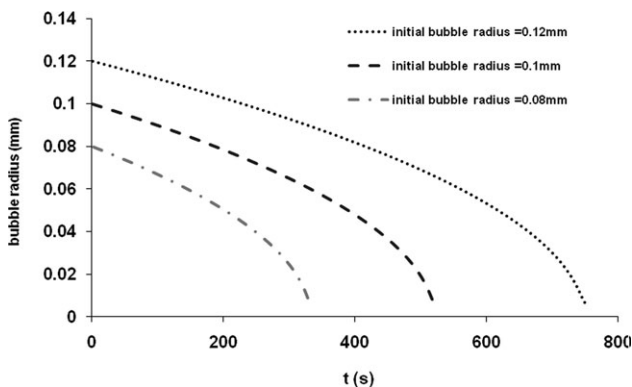


FIG. 15. The effect of initial bubble size on their life time and dissolution rate in PP melt.

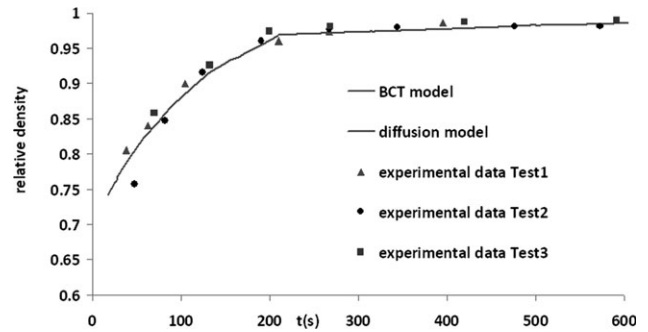


FIG. 16. Relative density of PVDF powder compact.

ment are the controlling parameters of initial bubble size. The polymer properties as surface tension and viscosity are the parameters that affect the densification rate, but their role on the initial bubble size is negligible. Molding condition (temperature) and polymer properties (viscosity, surface tension) are the parameters affecting bubble life time in the polymer. High-surface tension and temperature increase the diffusivity of gas into the polymer and decrease bubble life time. Proposed model considers the layer-by-layer nature of polymer powder densification. This model also related the powder bulk densification rate into the particles coalescence rate. As particle coalescence rate depends on material rheological properties and powder characterization, so this model relate powder densification rate to material rheological properties and powder characterization.

REFERENCES

1. C.H. Greene and R.F. Gaffney, *J. Am. Ceram. Soc.*, **42**, 271 (1959).
2. M.A. Rao and J.L. Throne, *Polym. Eng. Sci.*, **12**, 237 (1972).
3. P.Y. Kelly, *A Microscopic Examination of Rotomolded Polyethylene*, Du pont, Toronto, Canada (1981).
4. M. Kontopoulou and J. Vlachopoulos, *Polym. Eng. Sci.*, **41**, 155 (2001).
5. G.W. Scherer and T. Garino, *J. Am. Ceram. Soc.*, **68**, 216 (1985).
6. C.T. Bellehumeur and J.S. Tiang, *Polym. Eng. Sci.*, **42**, 215 (2002).
7. M. Kontopoulou and J. Vlachopoulos, *Polym. Eng. Sci.* **39**, 1189 (1999).
8. R.J. Crawford and J.A. Scott, *Plast. Rubber Process. Appl.* **7**, 85 (1987).
9. L. Xu and R.J. Crawford, *J. Mater. Sci.* **28**, 2067 (1993).
10. G. Gogos, *Polym. Eng. Sci.* **44**, 388 (2004).
11. A.G. Spence and R.J. Crawford, *Polym. Eng. Sci.*, **36**, 993 (1996).
12. E. Pérot, Ph.D. Dissertation, L'Institut National des Sciences Appliquées de Lyon, France (2006).
13. C.T. Bellehumeur, M. Kontopoulou, and J. Vlachopoulos, *Rheol. Acta.* **37**, 270 (1998).
14. J.E. Mark, Ed. *Polymer Data Handbook*, 2nd ed., Oxford University Press, New York.